Turbulence analysis with the Spectral Gas Puff Imaging diagnostic in the TJ-II stellarator

B.Ph. van Milligen[1], I. Voldiner[1], E. de la Cal[1], Arnold A. Alvarez[2], I.L. Caldas[2], Z.O. Guimarães-Filho[2] and the TJ-II Team

[1] *National Fusion Laboratory, CIEMAT, Avda. Complutense 40, 28040 Madrid, Spain.*
[2] *Instituto de Física, Universidade de São Paulo, São Paolo, SP, Brazil*

Introduction

In this work, we analyse data from the new Spectral Gas Puff Imaging diagnostic of the TJ-II stellarator. This diagnostic uses a fast camera to measure the intensity of three He emission lines, allowing the simultaneous reconstruction of the electron density and temperature (fluctuations) across a two-dimensional region in the plasma edge, with a time resolution that is relevant for turbulence analyses [1].

Experimental results

We analysed SGPI data from a typical TJ-II discharge in the standard magnetic configuration, with an ECR heating phase followed by an NBI phase. In the ECRH phase, the plasma is typically in electron root, while in NBI, it is in ion root. We selected time intervals in each phase, in order to facilitate comparison (Fig. 1). Mean fields of electron density and temperature are shown in Fig. 2. The apparent slight decay of the measured fields for $\rho < 0.75$ is due to line integration issues [2].

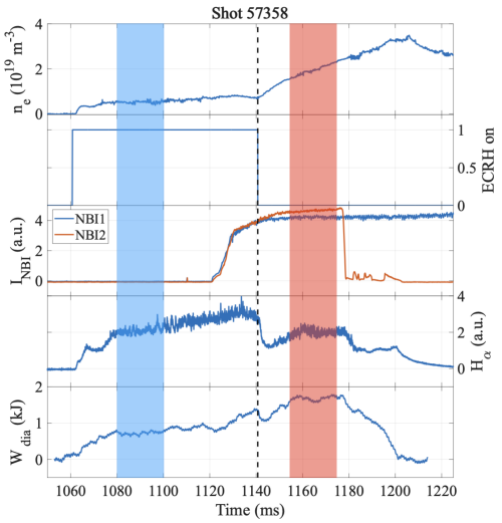

Fig. 1 – Discharge analysed. ECRH time window shaded in blue, NBI time window shaded in red.

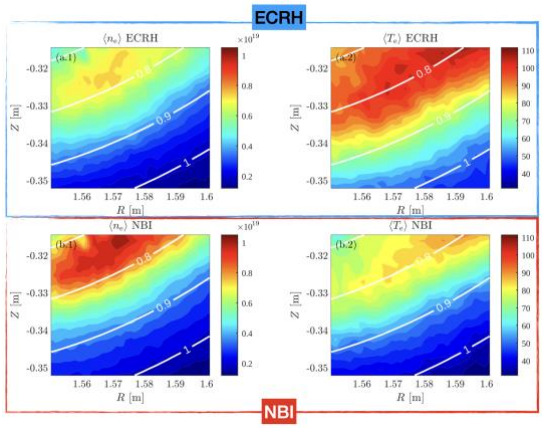

Fig. 2 – Mean electron density and temperature in each heating phase (ECRH and NBI). Calculated flux surfaces overlaid in white.

Summary radial statistics are shown in Fig. 3. Radial profiles of n_e and T_e are consistent with [1]. The normalized fluctuation level, RMS/mean, is higher for n_e than for T_e: ~20% for n_e vs. ~10% for T_e in the range $0.75 < \rho < 1$. The normalized fluctuation level is significantly increased during NBI. The cross-phase $\Delta\phi(n_e,T_e)$ was calculated using the Hilbert transform applied to the data for each pixel. The phase shows a very significant shift from phase $\Delta\phi \simeq 0$ in the far edge/SOL to phase $\Delta\phi \simeq \pm\pi$ further inward (in NBI). The graph shows $\cos(\Delta\phi)$ instead of $\Delta\phi$ itself, which changes from 1 ($\rho > 0.8$) to −1 ($\rho <$

0.8). The phase change is quite sharp and clearly occurs at a specific flux surface (ρ ≃ 0.8).

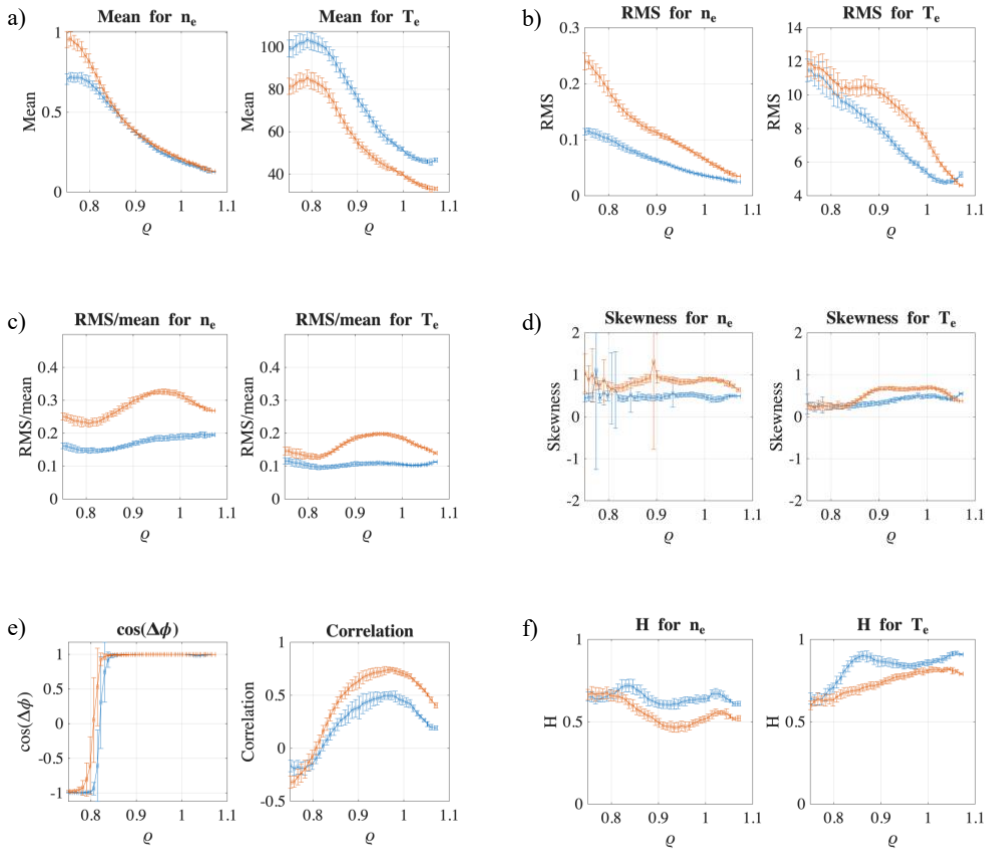

Fig. 3 – Summary radial plots of statistics (blue: ECRH, red: NBI). a) Mean value; b) Standard deviation; c) Normalized fluctuation amplitude; d) Skewness, e) Relative phase and correlation between n_e and T_e; f) Hurst exponent, H. All subplots except e) show these profiles for n_e on the left and for T_e on the right. Subplots a) and b) show n_e and RMS(n_e) in 10^{19} m^{-3}, T_e and RMS(T_e) in eV.

The cross correlation is consistent with the cross phase. The Hurst exponent H behaves differently for T_e and n_e, being generally higher for T_e than for n_e.

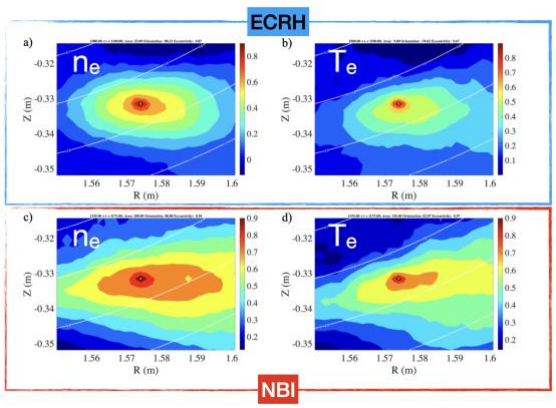

Fig. 4 - Auto-correlation between a reference point and the rest of the field of view.

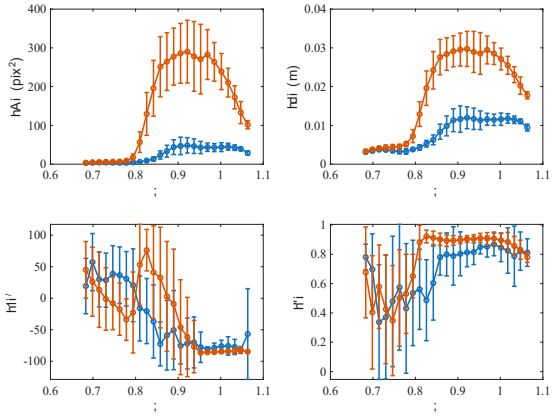

Fig. 5 – Radial profiles of blob quantifiers (ζ is the angle with the vertical in degrees, and ε is the eccentricity).

Fig. 4 shows a few typical auto-correlation graphs, revealing the average structure shape: elliptical and not aligned with the flux surfaces. Fig. 5 shows the resulting radial graphs of some parameters quantifying these structures. Again, significant changes between ECRH and NBI are observed, and radially at $\rho \approx 0.8$.

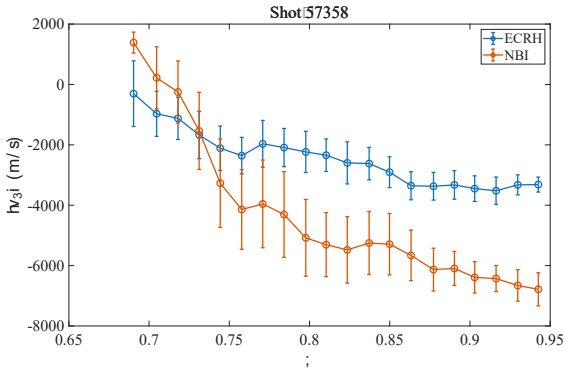

Fig. 6 – Apparent poloidal velocity

From the time-delayed cross correlation (of the n_e field), one can estimate the apparent structure velocity. Fig. 6 shows the poloidal component of this apparent velocity in ECRH and NBI. This velocity is a projection of the 3-dimensional velocity and is subject to various caveats (e.g., blobs moving outside the observation window). Nevertheless, in NBI the velocity becomes more negative in the edge and the velocity shear increases for $\rho < 0.75$, which matches other observations.

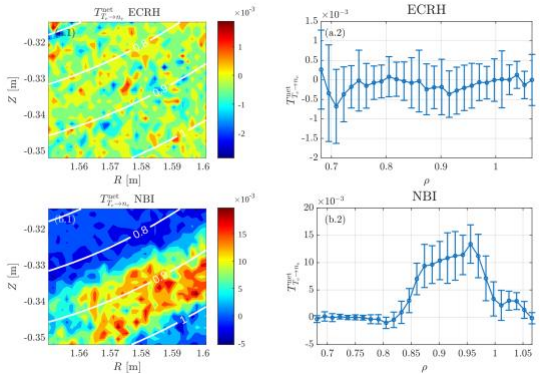

Above: Fig. 7 – Net transfer entropy from T_e to n_e.

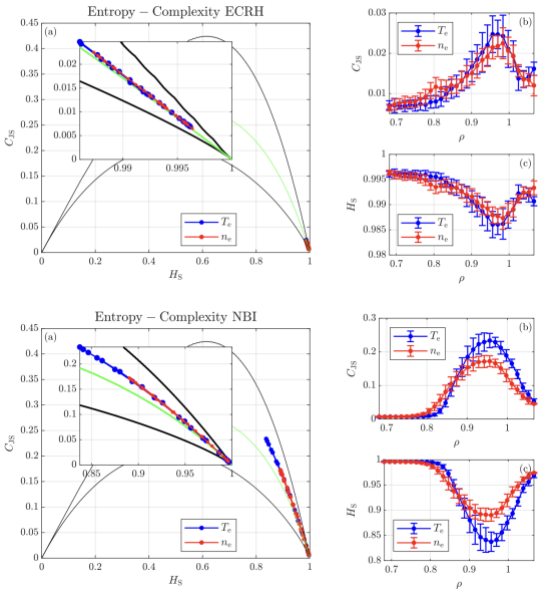

Right: Fig. 8 – Entropy-Complexity diagrams for both ECRH (top right) and NBI (bottom right). Note the large difference in vertical scale of subplots (b) and (c) between ECRH and NBI

Fig. 7 shows a calculation of the net Transfer Entropy from T_e to n_e. The Transfer Entropy quantifies information transfer (prediction capacity) between two fluctuating variables, which can be interpreted as a causal impact. While in ECRH, the net Transfer Entropy is essentially zero, significant values are detected in the NBI phase for $0.85 < \rho < 1$. This suggests the existence of a net information flow (causal influence) from T_e to n_e. A possible interpretation is that T_e is regulated by some mechanism (an ETG instability threshold?), and n_e follows. This would also be consistent with the relatively high value of the Hurst exponent found above for the T_e fluctuations.

Figure 8 shows the results of a Jensen-Shannon entropy–complexity analysis. This technique allows distinguishing between stochastic (random) and chaotic behaviour. The graphs shown in the subplots (a) shows that data are well away from the green line (corresponding to fractional Brownian or pink noise) and lie in a part of plane with non-trivial, complex and deterministic behaviour. In ECRH, the Complexity is small and the

Entropy is large, meaning that oscillations are close to random, consistent with [3]. In NBI, the Complexity is large and the Entropy is small in the range $0.85 < \rho < 1$.

Conclusions

SGPI is a promising new diagnostic for edge turbulence analyses. It provides direct access to 2-D n_e and T_e fields at turbulence-relevant sampling rates.

The above results detect significant changes between the ECRH phase (electron root) and the NBI phase (ion root).

In the interior region ($r < 0.8$), structures are small (~0.5 cm), while n_e and T_e are weakly correlated and in phase opposition. The small structure size could be related to the observed flow shear in this region.

In the edge region ($\rho < 0.8$), structures are large (~1 cm in ECRH to ~3 cm in NBI), while n_e and T_e are strongly correlated and in phase. The Jensen-Shannon Complexity-Entropy analysis detects nontrivial low-dimensional deterministic behaviour in the NBI phase. The Hurst exponent points to the presence of some self-regulation mechanism (critical gradient, ETG?) that is acting mainly on T_e. Indeed, the Transfer Entropy detects a causal information flow from T_e to n_e in the edge in the NBI phase.

The various changes associated with the $\rho \approx 0.8$ surface could be related to the presence of the 8/5 rational at roughly that position.

Acknowledgements

Research sponsored in part by the Ministerio de Ciencia e Innovación of Spain under project Nos. PID2021-124883NB-I00 and PID2022-137869OB-I00. This work has been carried out within the framework of the EUROfusion Consortium, funded by the European Union via the Euratom Research and Training Programme (Grant Agreement No 101052200 – EUROfusion). Views and opinions expressed are however those of the author(s) only and do not necessarily reflect those of the European Union or the European Commission. Neither the European Union nor the European Commission can be held responsible for them.

References

[1] I. Voldiner, E. de la Cal, B. van Milligen, and TJ-II Team. Spectroscopic gas puff imaging diagnostic for the measurement of two-dimensional electron density and temperature distributions. Plasma Physics and Controlled Fusion, 68(4):045017, 2026.

[2] B.Ph. van Milligen, I. Voldiner, E. de la Cal, Arnold A. Alvarez, I.L. Caldas, Z.O. Guimarães-Filho and the TJ-II Team. Turbulence analysis with the Spectral Gas Puff Imaging diagnostic in the TJ-II stellarator, PPCF (submitted, 2026)

[3] A. Alvarez et al. Edge Turbulence Dynamics Across Electron–Ion Root Transitions During ECRH Modulation Experiments in the TJ-II Stellarator. This conference